

EFFECTS OF GRAVITATIONAL FORCES ON SELF-PROPELLED DROPLET JUMPING

Figueiredo P.*, Kneer R. and Rohlf W.

*Author for correspondence

Institute of Heat and Mass Transfer,
RWTH Aachen University,
Germany,

E-mail: figueiredo@wsa.rwth-aachen.de

ABSTRACT

Hydrophobic or superhydrophobic surfaces are designated by a low wettability that gives rise to self-cleaning properties with applications such as non-wetting condensers or anti-icing coatings. One self-cleaning mechanism is self-propelled droplet jumping, which is the result of droplet coalescence on a superhydrophobic surface. Here, the release of surface energy allows for droplets jumping off the surface. For self-propelled droplet jumping, research is focused on jumping mechanisms, the energy budget of jumping droplets, and on the dependence of jumping velocities on substance and wetting properties. However, most studies are concentrated on analyzing the coalescence of droplets with no influence of gravity, which depending on droplet size, is rather an exception than the general case. Through three-dimensional simulations, this study analyses the fluid dynamics of droplet jumping upon binary droplet coalescence. The influence of gravitational forces is analyzed on jumping velocities, where lift-off regimes are bounded with Ohnesorge number and Bond number. As both are functions of droplet size, special care is given to describe size effects as a single parameter. The well-known small conversion efficiency for droplet jumping, where around 6% of the released surface energy is convertible into translational kinetic energy, is further reduced in presence of gravitational forces. Adhesion energy increases, since contact area increases as a consequence of the deformed droplet shape under gravitational effects. Interestingly, preliminary results show that for nearly inviscid flow maximum jumping is not achieved in the absence of gravity but in the case of $Bo \approx 0.1$. These findings can be used to complement existing models of dropwise condensation on superhydrophobic surfaces.

INTRODUCTION

On low adhesion surfaces, droplet coalescence can induce a translational motion directed away from the solid surface [12; 1]. Recently, droplet jumping has attracted renewed attention in the context of material sciences and the development of synthetic and natural superhydrophobic surfaces [1; 11; 3].

Figure 1 illustrates the different stages of droplet jumping. At the onset of coalescence, droplets form a capillary bridge, which

NOMENCLATURE

A	[m ²]	Area
Bo	[-]	Bond number
E	[J]	Energy
Oh	[-]	Ohnesorge number
r	[m]	Radius
t^*	[-]	Dimensionless time
U	[m/s]	Characteristic jumping velocity
u^*	[-]	Dimensionless velocity

Special characters

η	[-]	Jumping efficiency
θ	[-]	Contact angle
τ	[s]	Capillary-inertial time
σ	[J/m ²]	Surface tension
μ	[kg/m/s]	Viscosity

Subscripts

b	Bridge
C	Contact
s	Static
k	Kinetic
l	Liquid
$diss$	Dissipation
osc	Oscillation
g	Gravity
lg	Liquid-gas
ls	Liquid-solid
lim	Limit

extends due to capillary forces and results in an oscillatory motion. The solid surface breaks the axisymmetric motion accelerating the merged droplet away from the solid surface. Depending on the ratio of surface energy to viscous dissipation, the upward motion may cause droplets to detach from the solid surface.

The fluid dynamics of droplet coalescence on solid surfaces is governed by a balance of surface energy, kinetic energy, viscous dissipation and gravitational effects. During coalescence the overall droplet surface area is reduced and surface energy is released. On low adhesion surfaces and for vanishing viscous forces, the excess energy may propel the merged drop away from the solid surface. The energy balance for the case with two inviscid spherical droplets with radii r_0 on a surface with no adhesion gives a characteristic jumping velocity [1; 9; 8],

$$U = \sqrt{\frac{\sigma}{\rho_l r_0}}, \quad (1)$$

where σ is the surface tension and ρ_l the density of the liquid droplets. Unsteady motion is governed by the capillary-inertial time-scale of coalescence [6; 5]:

$$\tau = \sqrt{\frac{\rho_l r_0^3}{\sigma}} \quad (2)$$

By introducing capillary-inertial scaling from equation (1) and (2), coalescence-induced droplet jumping can be characterized in terms of dimensionless time scales $t^* = t/\tau$ and velocities $u^* = u/U$. Similarly, the influence of viscous damping can be given by the Ohnesorge number

$$\text{Oh} = \frac{\mu}{\sqrt{r_0 \rho_l \sigma}} \quad (3)$$

and finally the Bond describes the interrelation of gravity to surface tension

$$\text{Bo} = (\rho_l g r_0^2)/\sigma \quad (4)$$

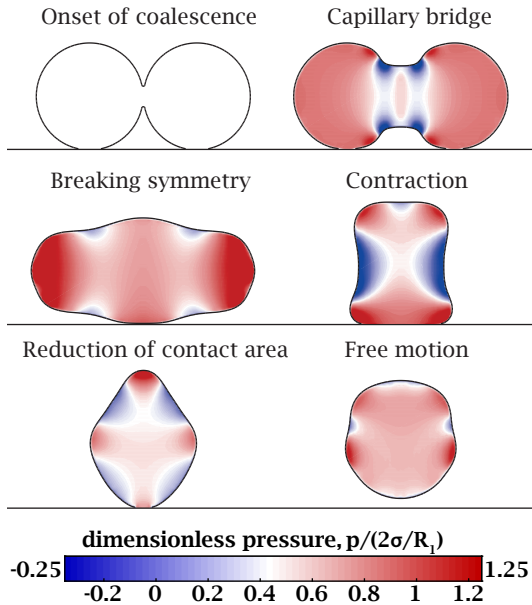


Figure 1. Mechanism of coalescence-induced droplet jumping. The coalescence of droplets leads to the release of surface energy, which is converted into translational motion. The static pressure field is scaled with the capillary pressure.

where μ is the dynamic viscosity of the droplet and g the gravitational acceleration. In this study, as we focus on the influence of gravity, we consider ($\text{Bo} \geq 0$). Finally, wall adhesion is described on the basis of contact angle θ . Figure 1 shows own three-dimensional simulation results providing a phenomenological picture of the jumping mechanism. In the first stage, the capillary bridge between the droplets extends as is known from droplet coalescence in free flow. In the second stage, the axisymmetric motion is broken as the capillary bridge reaches the wall, forcing the droplet into an upward motion. In the third stage, the droplet starts to contract, leading to further acceleration in upward direction. In the final stage, the upward motion reduces the contact area. If viscous dissipation and adhesive forces are dominating over inertia, the droplet loses its kinetic energy and adheres to the surface; otherwise, the droplet detaches and jumps off the superhydrophobic surface. In this sense, determination of the sessile droplet shape under gravity effect is crucial for accounting correctly surface adhesion.

Sessile Droplet Shape

On the onset of coalescence, the equilibrium shape of the two droplets in the absence of gravity is a spherical cap, which is the shape that minimizes the free energy of the system. In presence of gravity, with $\text{Bo} \gg 0$, the spherical shape is broken, and the equilibrium shape is a competition between gravity and surface tension. In the case $\text{Bo} \gg 0$ the determination of the axisymmetric equilibrium shape requires integration of a non-linear second-order differential equation, given by the Laplace equation, which describes the pressure difference across the surface of the droplet to its surface energy scaled by the curvature. To describe the equilibrium shape, an ellipsoidal droplet model is frequently adopted, also by limiting the analysis to perfect smooth surfaces [2]. In the present study, the model proposed by [10] was used to describe the sessile droplet shapes on the onset of coalescence. As mentioned before, self-propelled droplet jumping is influenced by adhesive forces, which in turn require determination of the contact line between the droplets and the surface.

Through numerical studies [10] and experimental observations [2] it is clear that in the presence of gravity, the flattening effect resulting from the body forces is to increase the contact area and decrease the height of the droplet. For values $\text{Bo} < 1$, the ellipsoidal approximation of a droplet shape is very satisfactory, even for higher contact angles [10]. In the present study a comparison was made between the predicted contact area using the ellipsoidal approximation and the simulated contact area and is presented in figure 2. There is a good agreement between predicted and simulated contact areas, specially in the lower Bond numbers which are subject of the present study. Determining a priori the sessile droplet shape allows to develop first hard conditions to bound the parameter space of droplet jumping. In this manner, no self-propelled droplet jumping is possible when the adhesion energy $\Delta E_{\text{adhesion}}$ needed to be overcome is higher than the release in droplet surface energy ΔE_{merge} .

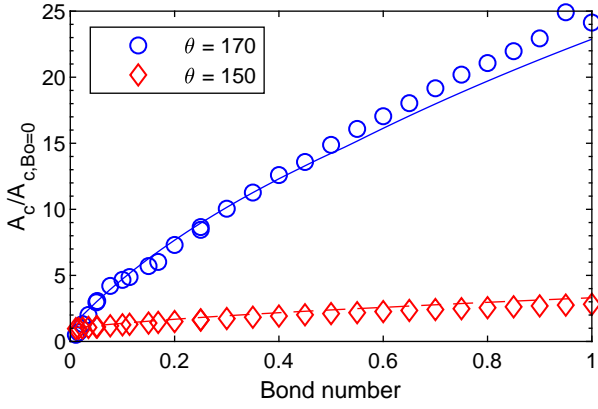


Figure 2. Comparison between the predicted contact area using the ellipsoidal approximation (-) and the computed contact area (o) for two different contact angles. The areas were made dimensionless with the contact area of a sessile droplet for under no gravity influence, $A_{c,B0=0}$.

STATIC ENERGY ANALYSIS

The released excess of surface energy in coalescence leads to a droplet motion (kinetic energy) and to an oscillation with droplet deformation (energy stored in surface energy). The total kinetic energy E_k is the result of the competition between the released surface energy ΔE_{merge} and the dissipation arising from the work of viscosity E_{vis} , both increase in $\Delta E_{\text{adhesion}}$ and gravitational potential energy ΔE_g ,

$$E_k = \Delta E_{\text{merge}} - E_{\text{visc}} - \Delta E_{\text{adhesion}} - \Delta E_g \quad (5)$$

The kinetic energy can be decomposed into translational and oscillatory components. As far as droplet jumping is concerned, the translational kinetic energy $E_{k,\text{trans}}$ is the only relevant part. Due to flow symmetry, there is no other translational motion than normal to the surface, which arises from the break of symmetry of the coalescence-induced motion. The oscillatory translational kinetic energy hinders the jumping motion, since energy is mainly dissipated by the internal liquid viscosity, hereafter accounted for in $E_{\text{diss,visc}}$. The translational kinetic energy, $E_{k,\text{trans}}$ can be written as

$$E_{k,\text{trans}} = \eta \Delta E_{\text{merge}} \quad (6)$$

introducing η as energy conversion efficiency, which is around 6% [8; 9; 13] for inviscid flow and superhydrophobic and smooth surfaces. The gravitational energy is related to the Bond number and the vertical variation of the centroid of the droplet $\Delta z^* = \Delta z/r_0$,

$$\Delta E_g^* = \text{Bo} \Delta z^* \quad (7)$$

By balancing the surface energies during the process of coalescence and jumping, a first hard condition under which droplet jumping may occur can be developed. For this, the surface and adhesion energy of three different static states are considered, illustrated in figure 3.

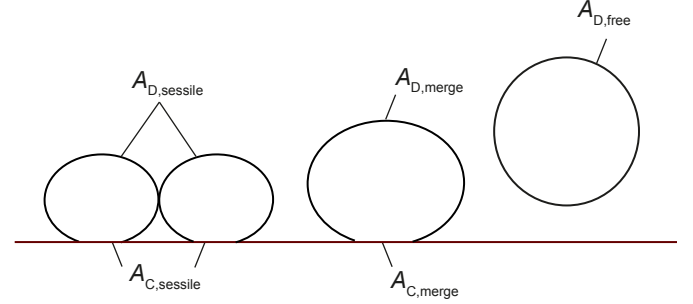


Figure 3. Three states for the static energy analysis.

In the first state, two sessile droplets are attached to the surface with a prescribed contact angle θ . In the second state, a stationary merged droplet and, finally in the third state, a detached droplet. The total liquid volume is equal in all three cases. As mentioned before, the presence of body forces flattens the sessile droplets against the surface, increasing the contact area. In the foregoing static analysis, an equilibrium droplet shape is assumed as predicted by an ellipsoidal approximation. During coalescence the released excess in surface energy is described by

$$\Delta E_{s,\text{merge}} = \sigma [\Delta A_{lg} - \Delta A_{ls} \cos(\theta)], \quad (8)$$

where ΔA_{lg} is the change in area between liquid (l) and gas (g) phase and ΔA_{ls} is the change in contact area between liquid and solid (s) phase. The released surface energy is partially converted into kinetic energy and leads to droplet motion. The remaining released surface energy leads to droplet deformation, thus energy is stored in the form of surface energy. Detaching the joint sessile drop after coalescence from the surface results in an increase in surface area, the energy difference between the sessile drop and the free drop is given by

$$\Delta E_{s,\text{adhesion}} = \sigma [A_{D,\text{sessile}} - A_{D,\text{free}} - A_{C,\text{sessile}} \cos(\theta)], \quad (9)$$

where the surface area of the sessile droplet and the contact area are equal to $A_{D,\text{merge}}$ and $A_{C,\text{merge}}$, respectively. The conservation of liquid volume is accounted for in all calculations

of droplet merging and droplet detachment. An absolute criterion for droplet jumping is given by $\eta \Delta E_{s, \text{merge}} > \Delta E_{s, \text{adhesion}}$, assuming that droplet jumping occurs with virtual zero translational kinetic energy. Figure 4 shows the ratio between the

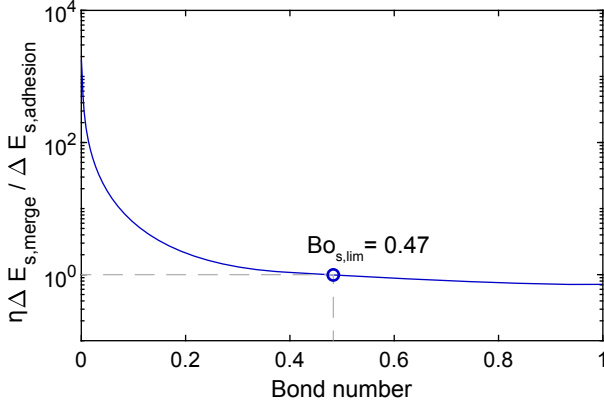


Figure 4. Relation of the excess in surface energy $\Delta E_{s, \text{merge}}$ to change the in adhesion energy $\Delta E_{s, \text{adhesion}}$ depending on Bond number and resulting from the static energy analysis, assuming an efficiency of $\eta = 6\%$, inviscid flow and contact angle $\theta = 170^\circ$.

energy of droplet merging and the adhesion energy of droplet detachment. In the presence of strong body forces (increasing Bo values), $\Delta E_{s, \text{merge}}$ is not sufficient for droplet jumping. Beyond $Bo = 0.47$, the available energy (surface energy released by merging droplets) is not enough for droplet detachment. Note that this approach of static energy balances assumes similar energy conversion and dissipation process to the case of binary coalescence without body forces. The coalescence efficiency $\eta = 6\%$ employed to predict the boundary for droplet jumping due to body forces, $Bo_{s, \text{lim}} = 0.47$, was obtained for cases $Bo \approx 0$. The validity of $\eta = 6\%$ for $Bo > 0$ will be assessed a posteriori. The present study aims to check if the portion of available excess surface energy converted into vertical translational energy remains constant. Additionally, since a large amount of the released energy results in droplet oscillation, not contributing to droplet detachment, the changes in the coalescence and oscillation flow patterns due to gravity have also to be analyzed. To do so, the phenomena is further studied using numerical simulations.

NUMERICAL SIMULATION

Coalescence-induced droplet jumping is described by an incompressible two-fluid flow, where the motion is governed by the Navier-Stokes equations. Interfacial forces originate from curvature only. At the three-phase contact line, a constant contact angle is assumed to restrict the number of influencing parameters. The numerical simulation of coalescence-induced droplet jumping is performed with a modified version of the volume-of-fluid (VOF) solver implemented in OpenFOAM. For coalescence-

induced droplet jumping, a cartesian mesh is used for spatial discretization with adaptive mesh refinement near the interface to ensure sufficient resolution without inflating overall computational cost. Time step is controlled dynamically to ensure the stability limits imposed by the Courant number and capillary time scales.

Kinematics of Jumping

The fundamental fluid dynamics of coalescence-induced droplet jumping is discussed next for nearly non-wetting and low-viscosity conditions of $Oh = 0.001$ and $\theta = 170^\circ$ under the influence of gravity $Bo = 0.2$. Two droplets are initialized in their steady state positions according the ellipsoidal equilibrium model [10]. The contours show the pressure field in figure 5, giving an intuitive illustration of the acting capillary forces and of traveling capillary waves. The jumping process is frequently divided into four stages: formation and expansion of the liquid bridge; acceleration of the merged droplet as a result of non-wetting surface reaction; droplet departure; and deceleration of the jumping droplet in the air due to friction and additionally (for the present case) gravity counteraction. In this study, the first three steps are of great interest, which focuses on the interactions between the droplets and the solid surface. At $t^* = 0$, the droplets were initialized next to each other with their edges overlapping, triggering the onset of coalescence. At the beginning of coalescence, a tiny liquid bridge between two droplets started to form. The expansion of the liquid bridge was driven by the surface tension and follows $r_b/r_0 \sim (t/t^*)^{1/2}$ [6; 5; 7].

On the other hand, as the capillary bridge expands, two capillary waves are induced and travel along the interface away from the bridge region. The waves are characterized by high and low pressure regions near the interface, which are noticeable in the pressure contours between $t^* = 0.14$ and $t^* = 0.43$. In stage (I) low interaction between the merged drop and the solid surface leads to near-zero vertical velocity, as seen in figure 6.

Due to strong body forces towards the surface, an instantaneous levitation of the droplet is not seen at $t^* = 0.57$, since gravity prevails over the inertia of the liquid bridge. As presented in figure 7, in the absence of gravity there is a pseudo droplet departure at $t^* = 0.55$.

Thereafter, the liquid bridge fully expands and reaches the surface at $t^* = 0.72$. The downward motion of the liquid was converted into upward motion due reaction of the surface, inducing droplet jumping. The break of vertical symmetry of the liquid bridge due to the presence of the substrate is the first acceleration mechanism for self-propelled droplet jumping. At $t^* = 1.4$ the capillary waves reach the sides of the merged drop and are reflected.

The returning capillary waves run towards the solid surface, which is the beginning of the second acceleration mechanism, at $t^* = 1.7$. The impinging wave is associated with strong curvatures and high pressures near the three-phase contact line as shown in figure 5, which induces further acceleration in wall-normal direction, as given in figure 6. Finally, the returning cap-

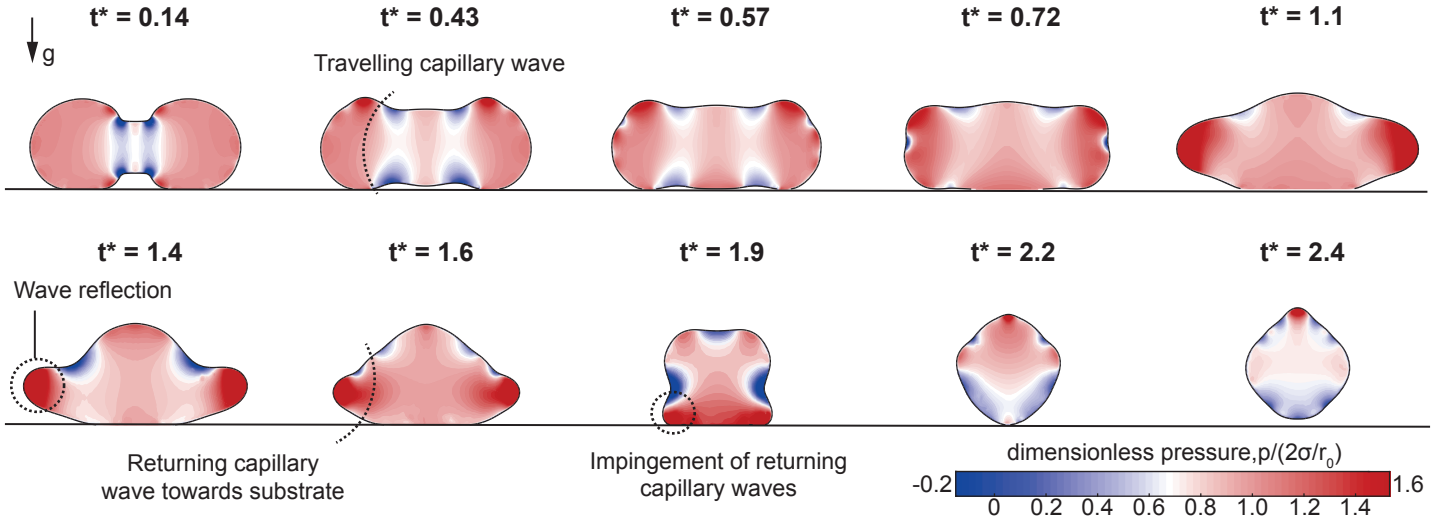


Figure 5. Time evolution of droplet shape for $Bo = 0.2$, $Oh = 0.001$ and $\theta = 170^\circ$. The contours in the symmetry plane show the static pressure (made dimensionless with the capillary pressure). Two acceleration mechanisms are identified: impact of the capillary bridge and impingement of capillary waves. The droplet detaches from the solid surface at $t^* \approx 2.35$, initiating free motion in the gas phase.

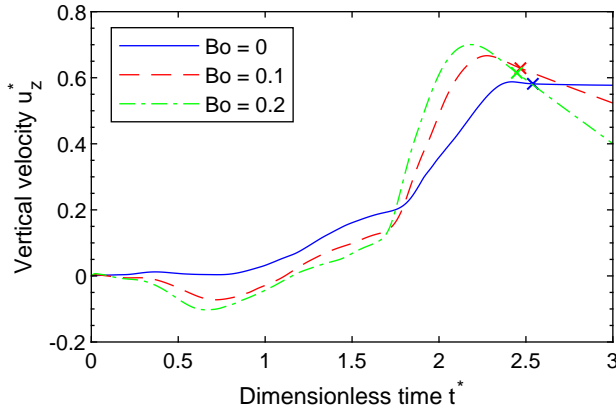


Figure 6. Transient vertical velocity and departure point (\times) for different Bo numbers.

illary waves collide with the solid surface, as seen at $t^* = 1.9$, causing a second acceleration mechanism due to surface reaction. Both capillary waves travel synchronously and both reflections impinge the solid surface simultaneously, since both droplets have the same size. Interestingly, this second acceleration mechanism droplet jumping is enhanced with increasing Bo . For inviscid flow, droplets jump off earlier and with higher vertical velocity in the cases with gravity ($Bo > 0$), than without gravity ($Bo > 0$) as seen in figure 6. Finally, the merged droplet jumps off the surface at $t^* \approx 2.35$.

Energetics of Jumping

To account for the influence of viscosity and gravity, a two-dimensional parameter space is considered, which contains Ohnesorge number, Oh , and Bond number, Bo . Since Ohnesorge

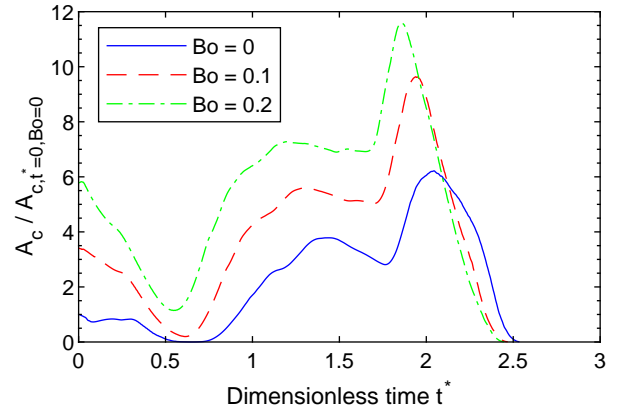


Figure 7. Transient contact area for different Bo numbers. The actual contact area A_c is divided by the initial contact area at $t^* = 0$ for neglecting gravity forces $A_{t^*=0, Bo=0}$ to highlight the influence of gravity.

and Bond number are functions of diameter, the Bond number Bo is varied with $BoOh^4$, similar to the work by [4]. Within this parameter space, the Ohnesorge number is the only size parameter and $BoOh^4$ is a substance property. While this modification is not motivated from physical considerations, it allows to describe size effects by one parameter only. In the following discussion Bo is not a size parameter for the reasons mentioned before. In order to present, compare and discuss the energetics of droplet jumping process, energies are normalized with σr_0^2 . The kinetic energy of the droplet is calculated by integrating the absolute velocity over the entire liquid volume. Change in surface adhesion is tracked analogously to equation 9. Figure 8 shows the

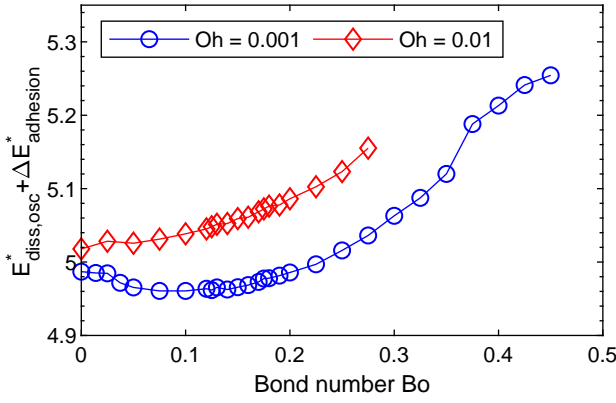


Figure 8. Competition of dissipating energy $E_{\text{diss,osc}}^*$ and change in adhesion energy before and after coalescence $\Delta E_{\text{adhesion}}^*$, for $\theta = 170^\circ$.

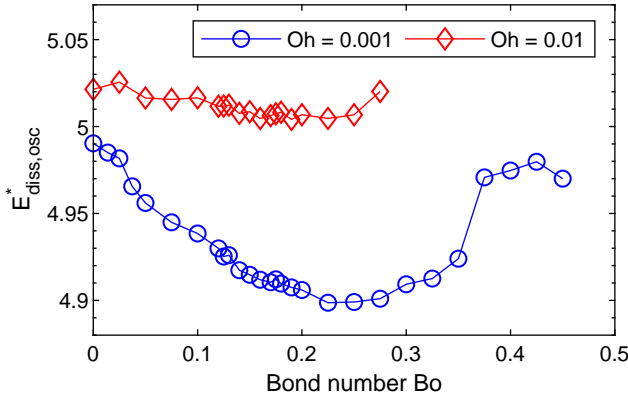


Figure 9. Energy dissipation for two different Oh numbers with increasing influence of gravitational force

competition of dissipating energy $E_{\text{diss,osc}}^*$ and change in adhesion energy before and after coalescence $\Delta E_{\text{adhesion}}^*$. For nearly inviscid flow, $\text{Oh} = 0.001$, increasing body forces do not hinder droplet jumping until $\text{Bo} \approx 0.2$. In the range $0.03 < \text{Bo} < 0.12$, droplet jumping is even enhanced due a decrease in energy dissipation, see figure 9. Droplet jumping was observed for $\text{Bo} < 0.45$ and for $\text{Bo} < 0.275$ for $\text{Oh} = 0.001$ and $\text{Oh} = 0.01$, respectively. As presented in figure 9, with increasing Bo leads to a reduction in viscous dissipation for $\text{Oh} = 0.001$ until $\text{Bo} \approx 0.35$. For $\text{Oh} = 0.01$, gravity has almost no influence on viscous dissipation. The decrease in viscous dissipation for nearly inviscid flow ($\text{Oh} = 0.001$), is explained by the influence of gravity on the traveling direction of returning capillary waves after its reflection during droplet oscillation ($t^* = 1.4$, see figure 5). Since both returning capillary waves travel towards the surface, surface reaction is increased leading to higher vertical velocity, as seen in

figure 6. As such, there is no efficiency loss due to gravity in droplet coalescence until $\text{Bo} \approx 0.2$ for nearly inviscid flow and $\theta = 170^\circ$, as seen in figure 8. For $\text{Bo} > 0.2$, adhesion forces become too strong and droplet jumping is hindered. The limiting Bo number is very close to the prediction ($\text{Bo}_{\text{s,lim}} = 0.47$) of the static energy balance presented in the previous section. The good agreement of both predicted and calculated limiting Bo numbers indicates that the efficiency of the self-propelled droplet jumping process is similar in the cases with and without gravity for inviscid flow. For the second case, increasing from $\text{Oh} = 0.001$ to $\text{Oh} = 0.01$, there is a slight increase in viscous dissipation due to the increasing ratio of viscous forces to surface tension, which explains the raise in $E_{\text{diss,osc}}^*$ for $\text{Bo} = 0$. More interestingly, viscous energy dissipation is not increased with increasing body forces. In figure 9 $E_{\text{diss,osc}}^*$ is nearly constant over Bo for $\text{Oh} = 0.01$.

CONCLUSION

In this study, the phenomenon of droplet jumping upon gravitational forces was analyzed by direct numerical simulations. Results show that the influence of gravity is twofold. For nearly inviscid droplets ($\text{Oh} = 0.001$), in the range $0.03 < \text{Bo} < 0.12$, droplet jumping is enhanced with gravity due to a decrease in energy dissipation. On the other hand, with increasing viscous dissipation, adhesion energy due to flattening of the droplet shape limits droplet jumping. The efficiency impairment is strengthened with increased viscous dissipation.

REFERENCES

- [1] J. B. Boreyko and C.-H. Chen. Self-propelled dropwise condensate on superhydrophobic surfaces. *Physical review letters*, 103(18):184501, 2009.
- [2] E. Y. Bormashenko. *Wetting of real surfaces*, volume 19 of *De Gruyter studies in mathematical physics*. De Gruyter, Berlin and New York, 2013.
- [3] X. Chen, R. S. Patel, J. A. Weibel, and S. V. Garimella. Coalescence-induced jumping of multiple condensate droplets on hierarchical superhydrophobic surfaces. *Scientific Reports*, 6(1):409, 2016.
- [4] Y. Cheng, J. Xu, and Y. Sui. Numerical investigation of coalescence-induced droplet jumping on superhydrophobic surfaces for efficient dropwise condensation heat transfer. *International Journal of Heat and Mass Transfer*, 95:506–516, 2016.
- [5] L. DUCHEMIN, J. EGGERS, and C. JOSSERAND. Inviscid coalescence of drops. *Journal of Fluid Mechanics*, 487:167–178, 2003.
- [6] J. EGGERS, J. R. LISTER, and H. A. STONE. Coalescence of liquid drops. *Journal of Fluid Mechanics*, 401:293–310, 1999.
- [7] R. T. Eiswirth, H.-J. Bart, A. A. Ganguli, and E. Y. Kenig. Experimental and numerical investigation of binary coalescence: Liquid bridge building and internal flow fields. *Physics of Fluids*, 24(6):062108, 2012.
- [8] R. Enright, N. Miljkovic, J. Sprittles, K. Nolan, R. Mitchell,

- and E. N. Wang. How coalescing droplets jump. *ACS nano*, 8(10):10352–10362, 2014.
- [9] F. Liu, G. Ghigliotti, J. J. Feng, and C.-H. Chen. Numerical simulations of self-propelled jumping upon drop coalescence on non-wetting surfaces. *Journal of Fluid Mechanics*, 752:39–65, 2014.
- [10] V. A. Lubarda and K. A. Talke. Analysis of the equilibrium droplet shape based on an ellipsoidal droplet model. *Langmuir : the ACS journal of surfaces and colloids*, 27(17):10705–10713, 2011.
- [11] C. Lv, P. Hao, Z. Yao, Y. Song, X. Zhang, and F. He. Condensation and jumping relay of droplets on lotus leaf. *Applied Physics Letters*, 103(2):021601, 2013.
- [12] M. Kollera and U. Grigull. Über das abspringen von tropfen bei der kondensation von quecksilber. *Wärme- und Stoffübertragung*, 1969(2):31–35.
- [13] J. Wasserfall, P. Figueiredo, R. Kneer, W. Rohlf, and P. Pischke. Coalescence-induced droplet jumping on superhydrophobic surfaces: Effects of droplet mismatch. *Physical Review Fluids*, 2(12):014, 2017.